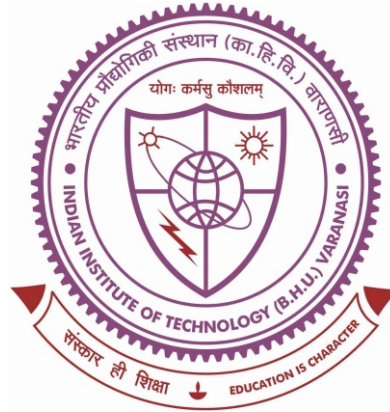


Static & Dynamic Characterization of Unreinforced and Reinforced Municipal Solid Waste (MSW Fines) for Geotechnical Applications



Thesis submitted in partial fulfillment for the
Award of Degree

Doctor of Philosophy

By

Parul Rawat

DEPARTMENT OF CIVIL ENGINEERING
INDIAN INSTITUTE OF TECHNOLOGY
(BANARAS HINDU UNIVERSITY)
VARANASI- 221005
INDIA

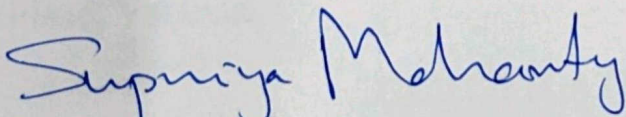
Roll No. 18061009

2023

CERTIFICATE

It is certified that the work contained in the thesis titled "**Static & Dynamic Characterization of Unreinforced and Reinforced Municipal Solid Waste (MSW Fines) for Geotechnical Applications**" by "**Ms. Parul Rawat**" has been carried out under my supervision and that this work has not been submitted elsewhere for a degree.

It is further certified that the student has fulfilled all the requirements of Comprehensive Examination, Candidacy, and State of the Art (SOTA) for the award of Ph.D. Degree.



Dr. Supriya Mohanty

Supervisor

Assistant Professor

Department of Civil Engineering

Indian Institute of Technology (BHU)

Varanasi, Uttar Pradesh, India-221005

Supervisor

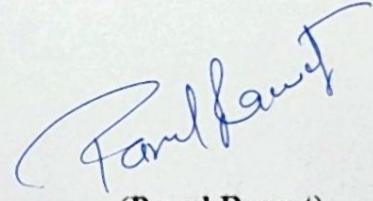
Department of Civil Engineering
Indian Institute of Technology, (BHU)
Varanasi-221005

DECLARATION BY THE CANDIDATE

I, **PARUL RAWAT**, certify that the work embodied in this thesis is my own bonafide work and carried out by me under the supervision of **Dr. SUPRIYA MOHANTY** from **July 2018 to January 2023** at the **Department of Civil Engineering, Indian Institute of Technology, (BHU) Varanasi**. The matter embodied in this thesis has not been submitted for the award of any other degree/diploma. I declare that I have faithfully acknowledged and given credits to the research workers wherever their works have been cited in my work in this thesis. I further declare that I have not willfully copied any other's work, paragraphs, text, data, results, *etc.*, reported in journals, books, magazines, reports dissertations, thesis, *etc.*, or available at websites and included them in this thesis and cited as my ownwork.

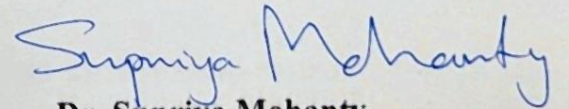
Date: 9.01.2023

Place: Varanasi


(Parul Rawat)

CERTIFICATE BY THE SUPERVISOR

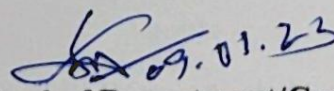
It is certified that the above statement made by the student is correct to the best of our knowledge.



Dr. Supriya Mohanty
(Supervisor)

Assistant Professor
Department of Civil Engineering
IIT (BHU), Varanasi-221005
Supervisor

Department of Civil Engineering
Indian Institute of Technology, (BHU)
Varanasi-221005


Signature of Head of Department/Coordinator of School
"SEAL OF THE DEPARTMENT/SCHOOL"

जानपद अभियांत्रिकी विभाग
Department of Civil Engineering
भारतीय प्रौद्योगिकी संस्थान (बी.एच.यू.)
Indian Institute of Technology, (BHU)
Varanasi-221005

COPYRIGHT TRANSFER CERTIFICATE

Title of the Thesis: **Static & Dynamic Characterization of Unreinforced and Reinforced Municipal Solid Waste (MSW Fines) for Geotechnical Applications**

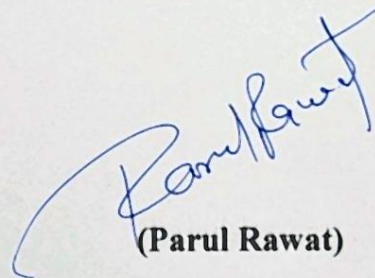
Name of the Student: **Ms. Parul Rawat**

Copyright Transfer

The undersigned hereby assigns to the Indian Institute of Technology (Banaras Hindu University) Varanasi all rights under copyright that may exist in and for the above thesis submitted for the award of the DOCTOR OF PHILOSOPHY.

Date: 3.01.2023

Place: Varanasi



(Parul Rawat)

Note: However, the author may reproduce or authorize others to reproduce material extracted verbatim from the thesis or derivative of the thesis for the author's personal use provided that the source and the Institute's copyright notice are indicated.

DEDICATED TO MY PARENTS

(Mr. Sanjay Singh Rawat and Mrs. Pratibha Rawat)

ACKNOWLEDGEMENT

This is the most difficult part of the thesis for me to write, I don't think a mere thanks could justify my emotions and gratitude for the people who have been through with me in my Ph.D. journey. Above all, I bow down to my "Ishta-Devata", the divinity that resides within me and every living creature.

This thesis would not be possible without the guidance of my supervisor, Dr. Supriya Mohanty, Civil Engineering Department, IIT(BHU), Varanasi. Although she is excellent at her job, she also inspires me personally and professionally about what it means to be an independent woman. I will be eternally grateful to her for inspiring, directing, and redirecting me, especially during the difficult Covid-2019 phase.

Being privileged to be a part of this century-old institute, I would like to express my sincere gratitude to the institute, IIT (BHU), and our civil engineering department. I would like to thank the Head of the Civil Engineering Department, Indian Institute of Technology (BHU), Varanasi, for providing all the facilities related to my research work. I wish to extend my sincere gratitude towards my RPEC members, Dr. Medha Jha as an internal expert and Dr. Chandna Rath as an external expert, for their help, valuable suggestions, and encouragement during the entire research work. I wish to express my deep regards to, Prof. Arun Prasad, Dr. Bala Ramudu Paramkusam, Dr. Suresh Kumar, and Dr. Manash Chakraborty for their unconditional support at every moment during the progress of my research. I also extend my heartfelt regards to all the faculty members of the Civil Engineering Department. I am also grateful to our laboratory staff, Basanta Prasad sir, Netra Pal sir and Deepak bhaiya for the assistance extended to them from time to time

during this research work. I am very thankful to Sanjay bhaiya for his assistance in lab work even during the odd hours of the day.

There are numerous people in my whole Ph.D. journey whom I would like to thank and who have touched my life in various ways. I'd like to thank my small geotechnical lab family, which includes Ankita mam, Deepjyoti mam, Rashmi mam, Manish sir, Shivani mam, Jayanti mam, Abhay sir, Niteesh sir, Sourav sir, Surya sir, Amit Kumar Ram, Amit Singh, Mayank Nishant, Munni Pradeep, Sanjoli, and Gaurav. I am grateful to some of my transportation division colleagues, Mohit, Mayank, Vivek, Nirmal, and Saroj, who were always willing to assist and offer research suggestions. There are a few friends who have personally motivated me, and without them, this Ph.D. journey would be incomplete. I would like to thank Ankit sir, Shreyansh, Ranveer, Lillian, Ria, Shreyashi, Poonam, Neetu, Priyanka, and Numa for simply being there for me during my odd days. I am extremely grateful to Ravi Kishore Reddy for directing and assisting me during my early Ph.D. days. I am grateful to Amit Kumar Ram for consistently motivating me for my research, from sharing research ideas to lab trials, success, and failure. Your encouragement has made this journey much easier for me. I'd like to thank Arun Kaintura for his time and assistance with the machine learning section, which would not have been possible without him.

Finally, I am thankful for my family's faith, patience, encouragement, blessings, and love. I am blessed with parents who have always supported my decision and a brother who gives me the strength to persevere in the face of adversity; I will be eternally grateful to them. My last thank would be to Devi (my pet), who restores my faith and shows that life is simple, we just make it complicated.

Date:

Place: Varanasi

Parul Rawat

ABSTRACT

Municipal solid waste (MSW) management is a leading challenge for humans currently. As we not only have to deal with the daily generated waste but also must find the solutions for already generated waste which still lying somewhere on the earth's surface. Landfilling which use to be the most viable option to get rid of our waste is no longer an acceptable disposal option left. Poor waste management and increasing waste generation have become environmental and health hazards. Now, this piled-up waste from decades in these landfills causes an alarming situation and can't be ignored. Other than sanitary landfills there are numerous unsanitary landfills and open dump sites which create more dangerous situations in the environment. One of the ways to deal with it could be extracting the waste from the landfills and recirculating the material and land cost in the economy, through enhanced landfill mining techniques. The most abundantly excavated material from sanitary landfills or open dump sites is the municipal solid waste (MSW) fine fractions which consist of more than 50% of the waste composition. These fine fractions also called "MSW fines/soil-like material" have the potential to be used as a bulk replacement for construction/geomaterials. Before this material can be used in bulk in fields as geomaterials in structures, it is important to check the behaviour of the considered material under realistic loading conditions (monotonic or dynamic). The heterogenic characteristic of the MSW is the major factor that influences all the other parameters and makes this material more unpredictable and challenging to reuse. The material characteristic of the MSW is very specific to the site it has been collected (origin of the waste), so it requires specified pilot projects to deal with the waste locally. The data from these pilot projects can be

further helpful to predict or model general geotechnical parameters (static or dynamic). Contributing to this objective a comprehensive experimental program has been planned. The MSW fines (particle size less than 4.75 mm) which contribute to the major portion of the decomposed waste and closely resemble the soil have been the focus of the study. The sample was collected from the local site Ramana in Varanasi. After segregation and processing, about 60% of waste was characterized as MSW fines. The basic physical, chemical, and geotechnical characterization of the waste categorize the MSW fines as lightweight, non-plastic silty sand-type material with good shear strength properties (cohesion and friction angle from 31.37 to 42.19 kPa and 26.69° to 30.74°, for relative compaction of 95 to 99% respectively) with an organic content of 5.9% and slight acidic behaviour. The study on MSW fines has been continued under static and cyclic loading conditions for unreinforced and reinforced categories. A set of 100 strain-controlled cyclic triaxial tests under consolidated undrained conditions were performed to study the cyclic behaviour of the considered MSW fines. The sensitivity of different parameters (relative compaction, effective confining pressure, cyclic shear strain, and loading frequency) on dynamic properties (dynamic shear modulus (G) and damping ratio (D)) of the MSW fines was evaluated. The MSW fines were reinforced with randomly distributed fibers which were also part of the waste collected from another site Karsada, Varanasi. These fibers were mixed to the MSW fines in 0.5, 1, 2, 4, 8, and 10%. The static and dynamic strength of the composite mix was evaluated to find the optimum percentage of fiber content in the mix. Through static strength tests, the optimum fiber content can be decided as 8%. But, the improvement in dynamic shear strength can't be seen as governed by the dynamic shear modulus of the material. The inclusion of fibers enhances the damping parameter of the MSW fines and can be used as shock absorbers but does not help in excess pore water pressure dissipation. It

can be concluded from the results that under static conditions, these waste fibers work satisfactorily and can be used as backfill or embankment material but has limited applications in high seismic zones.

Moreover, the small-strain shear modulus of unreinforced and fiber-reinforced MSW fines was evaluated through the laboratory bender element apparatus. The data evaluated from the laboratory tests were further used to develop empirical correlations for the unreinforced and fiber-reinforced MSW fines. Based on the experimental test results, the excess pore water pressure (r_u) model for the fiber-reinforced MSW fines was established. A cubic polynomial model was applied to correlate the normalized small-strain shear modulus (G_R/G_{UR}) and normalized shear strength (τ_R/τ_{UR}) of the reinforced and unreinforced MSW fines. Nonlinear models were fitted for the normalized shear modulus and damping ratio with cyclic shear strain for both the unreinforced and reinforced MSW fines. Further, the dynamic shear modulus data obtained from the cyclic triaxial tests of the unreinforced and reinforced MSW fines was used for the prediction model of MSW fines (dynamic shear modulus) through two machine learning techniques, i.e., Artificial neural network (ANN) and Gaussian process regression (GPR). The GPR model predicts better results for the dynamic shear modulus of unreinforced and reinforced MSW fines. The sensitivity analysis of the considered parameters on the dynamic shear modulus of MSW fines also correlated with the experimental results.

TABLE OF CONTENTS

CERTIFICATE	i-iii
DEDICATION	iv
ACKNOWLEDGEMENT	v-vi
ABSTRACT	vii-ix
TABLE OF CONTENTS	
LIST OF FIGURES	xvii
LIST OF TABLES	xxv
NOMENCLATURE	xxvii-xxxiv
CHAPTER-I INTRODUCTION	1
1.1 GENERAL BACKGROUND	1
1.1.1 Scenario of Waste Generation	1
1.1.2 Solid Waste Management (SWM) in India	5
1.1.3 Landfill Mining	10
1.2 AN OVERVIEW AND PROBLEM IDENTIFICATION	12
1.3 OBJECTIVES	14
1.4 SCOPE OF THE STUDY	14
1.5 ORGANIZATION OF THE THESIS	15
CHAPTER-II REVIEW OF LITERATURE	19
2.1 INTRODUCTION	19
2.2 CHARACTERIZATION STUDIES OF MSW FINES	20
2.2.1 Characterization of Landfill-Mined Waste	20
2.2.1.1 Indian Landfill Studies	21
2.2.1.2 Landfill Studies Around the World	22
2.2.2 Physico-Chemical Characterization of MSW Fines	35
2.2.3 Geotechnical Characterization of MSW Fines	49
2.3 DYNAMIC CHARACTERIZATION STUDIES OF MSW	66
2.4 STUDIES ON REINFORCED MSW	78
2.5 POTENTIAL RE-USABILITY AND CHALLENGES IN USING SOIL-LIKE WASTE/MSW FINE FRACTION	80
2.5.1 MSW Compost/Soil Conditioner	82
2.5.2 Reusability as Landfill Cover	83
2.5.3 Engineered Fill Material	84
2.5.4 Construction Material	86
2.6 TREATMENTS REQUIRED BEFORE FIELD APPLICATION	88
2.7 SUMMARY	92
CHAPTER- III MATERIALS, EXPERIMENTAL PROGRAM, METHODS, AND TEST PROCEDURES	93
3.1 INTRODUCTION	93
3.2 SOURCE OF MATERIALS USED	93
3.2.1 MSW Fines	93

3.2.2	Fibers	94
3.3	TESTING PROGRAM	94
3.3.1	Sample Collection and Segregation of Waste	94
3.3.1.1	MSW Fines	96
3.3.1.2	Fibers	96
3.3.2	Laboratory Study	99
3.3.2.1	Morphology, Mineralogy, and Chemical Characteristics Tests	102
3.3.2.1.1	Scanning Electron Microscope (SEM) Test	102
3.3.2.1.2	pH	102
3.3.2.1.3	Organic Content	103
3.3.2.1.4	Total Dissolved Solids (TDS)	103
3.3.2.1.5	Chloride Content	104
3.3.2.1.6	Total Dissolved Sulphate	104
3.3.2.1.7	Colour Unit Test	104
3.3.2.1.8	X-ray Diffraction (XRD) Test	104
3.3.2.1.9	X-ray Fluorescence (XRF) Test	105
3.3.2.2	2 Geotechnical Characterization Tests	105
3.3.2.2.1	MSW Fines	106
3.3.2.2.1.1	Grain size distribution	106
3.3.2.2.1.2	Atterberg limit test	106
3.3.2.2.1.3	Compaction test	106
3.3.2.2.1.4	Compressibility characteristics	106
3.3.2.2.1.5	Permeability test	107
3.3.2.2.1.6	Unconfined compression strength test (UCS)	107
3.3.2.2.1.7	Triaxial tests	107
3.3.2.2.1.8	California bearing ratio (CBR) test	109
3.3.2.2.2	Fiber-Reinforced MSW Fines	109
3.3.2.2.2.1	Compaction test	109
3.3.2.2.2.2	Compressibility characteristics	109
3.3.2.2.2.3	Triaxial tests	110
3.3.2.3	Strain Controlled Cyclic Triaxial Tests	111
3.3.2.3.1	Testing Equipment	115
3.3.2.3.2	Test Procedure	117
3.3.2.4	Bender Element Test	120
3.3.2.4.1	Testing Equipment	120
3.3.2.4.2	Test Procedure	123
CHAPTER- IV LABORATORY TEST RESULTS AND DISCUSSION		127
4.1	INTRODUCTION	127
4.2	STATIC LABORATORY TEST RESULTS	127
4.2.1	Morphology, Mineralogy and Chemical Characteristics	128
4.2.1.1	pH	128

4.2.1.2	Organic Content	128
4.2.1.3	Total Dissolved Solids	128
4.2.1.4	Chloride and Total Dissolved Sulphate Content	129
4.2.1.5	Colour Unit Test	129
4.2.1.6	Elemental/ Compound Analysis	129
4.2.1.7	Scanning Electron Microscope (SEM) Test	132
4.2.2	Geotechnical Characterization of MSW Fines	135
4.2.2.1	Grain Size Analysis	135
4.2.2.2	Specific Gravity	137
4.2.2.3	Atterberg Limit	137
4.2.2.4	Compaction Characteristics	137
4.2.2.5	Compressibility Characteristics	138
4.2.2.6	Permeability Characteristics	139
4.2.2.7	CBR Test	140
4.2.2.8	UCS Test	141
4.2.2.9	Static Triaxial Tests	142
4.2.3	Fiber-Reinforced MSW Fines	145
4.2.3.1	Compaction Characteristics of Fiber-Reinforced MSW Fines	146
4.2.3.2	Compressibility Characteristics of Fiber-Reinforced MSW Fines	146
4.2.3.2.1	Compressibility Parameters	147
4.2.3.2.2	Determination of Coefficient of Consolidation	151
4.2.3.3	Shear Strength Behaviour of Fiber-Reinforced MSW Fines	156
4.2.3.3.1	Unconsolidated Undrained Triaxial Test on MSW Fine Samples (Diameter: 38mm; Height:76mm)	156
4.2.3.3.2	Triaxial Test on MSW Fine Samples (Diameter: 50mm; Height:100mm)	159
4.3	DYNAMIC LABORATORY TEST RESULTS	161
4.3.1	Strain Controlled Cyclic Triaxial Test on Unreinforced MSW Fines	162
4.3.1.1	Cyclic Behaviour of Compacted MSW Fines	162
4.3.1.1.1	Variation of Deviator Stress, Pore Water Pressure, and Mean Effective Stress with Number of Cycles	162
4.3.1.1.2	Variation of Deviator Stress with Axial Strain and Mean Effective Stress	169
4.3.1.2	Liquefaction Potential of Compacted MSW Fines	173
4.3.1.3	Dynamic Properties of Compacted MSW Fines	175
4.3.1.3.1	Effect of Loading Frequency on Dynamic Properties of Compacted MSW Fines	175
4.3.1.3.2	Effect of Confining Pressure on Dynamic Properties of Compacted MSW Fines	177
4.3.1.3.3	Effect of Relative Compaction on Dynamic Properties of Compacted MSW Fines	179

4.3.1.3.4	Effect of Strain Amplitude on Dynamic Properties of Compacted MSW Fines	181
4.3.1.4	Degradation Index of Compacted MSW Fines	185
4.3.2	Dynamic Characterization of Fiber-Reinforced MSW Fines	188
4.3.2.1	Effect of FC on Cyclic Strength Parameter “G” of Fiber-Reinforced MSW Fines	188
4.3.2.2	Degradation Index of Fiber-Reinforced MSW Fines	191
4.3.2.3	Effect of FC on Cyclic Strength Parameter “D” of Fiber-Reinforced MSW Fines	193
4.3.2.4	Effect of FC on r_u (excess pore water pressure ratio) of Fiber-Reinforced MSW Fines	194
4.3.3	Shear Wave Velocity Determination Through Bender Element Analysis for Unreinforced and Reinforced MSW Fines with Fibers	197
4.3.3.1	Consideration of Parameters for Bender Element Test	197
4.3.3.2	Effect of Considered Parameters on Shear Wave Velocity (V_s)	198
4.3.3.2.1	Effect of Excitation Frequency (f) on V_s	198
4.3.3.2.2	Effect of Relative Compaction (R_c) on V_s	202
4.3.3.2.3	Effect of Confining Pressure (σ_c) on V_s	203
4.3.3.2.4	Effect of Fiber Content (FC) on V_s	205
4.3.3.2.5	Effect of Saturation on V_s	206
4.3.3.3	Comparison of Present Study Results with Past Literature	208
4.4	SUMMARY	210
CHAPTER- V CORRELATION STUDIES		213
5.1	INTRODUCTION	213
5.2	PORE WATER PRESSURE RATIO (r_u) MODEL FOR FIBER-REINFORCED MSW FINES	212
5.3	CORRELATION BETWEEN SMALL STRAIN SHEAR MODULUS (G_{max}) WITH SHEAR STRENGTH (τ) FOR FIBER REINFORCED MSW FINES	218
5.4	PREDICTION MODEL FOR DISSIPATED ENERGY OF UNREINFORCED AND REINFORCED MSW FINES AT LIQUEFACTION	220
5.4.1	Energy Method	220
5.4.2	Linear Regression Model for Dissipated Energy of Unreinforced MSW Fines at Liquefaction	223
5.4.3	Non-Linear Regression Model for Dissipated Energy of Reinforced MSW Fines at Liquefaction	224
5.5	CORRELATIONS BETWEEN NORMALIZED SHEAR MODULUS AND CYCLIC SHEAR STRAIN OF UNREINFORCED AND REINFORCED MSW FINES	226
5.6	CORRELATIONS BETWEEN DAMPING RATIO AND CYCLIC SHEAR STRAIN OF UNREINFORCED AND REINFORCED MSW FINES	231
5.7	LIMITATIONS OF THE PRESENTED CORRELATIONS	236
5.8	SUMMARY	236

CHAPTER- VI	PREDICTION OF DYNAMIC SHEAR MODULUS OF UNREINFORCED AND REINFORCED MSW FINES: MACHINE LEARNING APPLICATION	239
6.1	INTRODUCTION	239
6.1.1	ML Applications in Constitutive Modeling of Soils	241
6.2	PROBLEM SETTING	242
6.2.1	Prediction Models	243
6.2.1.1	Artificial Neural Network (ANN)	243
6.2.1.2	Gaussian Process Regression	245
6.2.1.3	Sensitivity Analysis	246
6.3	RESULTS AND DISCUSSION	247
6.3.1	Test Setup	247
6.3.2	Prediction Using Artificial Neural Network	248
6.3.3	Prediction Using Gaussian Process Regression	250
6.3.4	Sensitivity Analysis	252
6.4	SUMMARY	252
CHAPTER- VII	CONCLUSIONS AND FUTURE SCOPE	255
7.1	SUMMARY AND CONCLUSIONS	255
7.1.1	Geotechnical Laboratory Test Results	256
7.1.2	Cyclic Triaxial and Bender Element Laboratory Test Results	257
7.1.3	Correlations and Prediction Model Study Results	259
7.2	LIMITATIONS AND SCOPE FOR FUTURE WORK	260
7.2.1	Limitations	260
7.2.2	Scope for Future Work	260
	REFERENCES	263
	LIST OF PUBLICATIONS	313
	APPENDIX-A GEOSYNTHETIC REINFORCED MSW FINES	317
A.1	INTRODUCTION	317
A.2	MATERIAL PROPERTIES	317
A.3	EXPERIMENTAL STUDY	319
A.3.1	Testing Program	319
A.3.2	Sample Preparation	319
A.4	EXPERIMENTAL RESULTS AND DISCUSSION	321
A.4.1	Strength Performance of Reinforced MSW Fines under Static Loading Condition	321
A.4.2	Shear Strength Behaviour of Geotextile Reinforced MSW Fines	323
A.4.3	Shear Strength Behaviour of Geonet Reinforced MSW Fines	324
A.4.4	MSW Fines–Geosynthetic Strength Ratio	329
A.4.5	Strength Performance of Geosynthetic Reinforced MSW Fines under Cyclic Loading Condition	330
A.4.6	Comparative Analysis of Strength Under Static and Cyclic Loading Conditions	337
A.5	SUMMURY	339

LIST OF FIGURES

Figure No.	Description	Page No.
1.1	Top 20 waste generating countries with their GDP	4
1.2	Waste composition of (a) world (b) India	4
1.3	Indian landfill data (Source@ CPCB annual report (2019-20))	9
1.4	Indian solid waste management data (Source@ CPCB annual report (2019-20))	10
2.1	Cyclic triaxial test results and comparison with literature: (a) normalized shear modulus reduction curve (b) material dumping curve as a function of shear strain. (Source @ Zekkos et al. 2008)	70
2.2(a)	Plot of the variation of shear wave velocity (V_s) of MSW landfills with depth (z). (Source @ Choudhury and Savoikar 2009)	71
2.2(b)	Plot of the variation of normalized shear modulus (G/G_{max}) of MSW landfills with the percentage cyclic shear strain. a for clay; b for peat; c lower bound; d upper bound; e average values; f recommended (upper bound); g for 100% composition of waste of particle size smaller than 20 mm; h for 62–75% composition of waste of particle size smaller than 20 mm; i for 8–25% composition of waste of particle size smaller than 20 mm. (Source @ Choudhury and Savoikar 2009)	72
2.2(c)	Plot of the variation of the material damping ratio of MSW landfills with the percentage cyclic shear strain. a for clay; b for peat; c lower bound; d upper bound; e recommended (lower bound); f average values; g for 100% composition of waste of particle size smaller than 20 mm; h for 62–75% composition of waste of particle size smaller than 20 mm; i for 8–25% composition of waste of particle size smaller than 20 mm. (Source @ Choudhury and Savoikar 2009)	73
2.3	Potential use and considered treatments for MSW fine fraction	91
3.1	Location map of the sample collection sites	95
3.2	Cycle showing collection and segregation of MSW fine fractions	97
3.3	(a) 4 mm rejected sample collected from site-2, Karsada waste to energy plant, Varanasi; (b) air-blowing method for separating	98

	fibers from waste; and (c) heterogeneous fiber mix separated from the waste	
3.4	Photographic view of the strain-controlled cyclic triaxial testing equipment	116
3.5	Stages of sample preparation and mounting for cyclic triaxial test	119
3.6	Schematic of typical hysteresis loop	120
3.7	Bender element apparatus setup	122
3.8	Bender element attached to the triaxial cell	122
3.9	A typical input and output wave presented on oscilloscope display	123
3.10	Stages of sample preparation and mounting for bender element test	124
3.11	Testing program flow chart for the bender element test	124
4.1	Colour of leachates noticed from MSW fines	129
4.2	(a) EDX spectral image (b) X-ray diffraction pattern (c) Percentage of compounds by XRF (X-ray fluorescence spectroscopy) for MSW fines	130
4.3	Scanning electron micrographs of MSW fraction below 75 microns at magnification of (a) 1.00 kX; (b) 500X; (c) 5.00 kX; and (d) 10.00 kX	133
4.4	Grain size distribution curve of MSW sample (site 1) collected from field and finer portion used as MSW fines (below 4.75 mm)	136
4.5	Typical images of particles of MSW retained on (a) 2 mm; (b) 1 mm; (c) 425 micron; (d) 150 micron; (e) 90 micron; and (f) 75 micron IS sieve	136
4.6	Compaction curve for the MSW fines sample	138
4.7	(a) Variation of compression index (C_c); (b) coefficient of consolidation (C_v) with increase in percentage of R_C ; (c) variation of void ratio with applied stress at different R_C ; and (d) variation of permeability with increase in percentage of R_C of MSW fine samples.	139
4.8	(a) Load versus deformation graph for unsoaked and soaked CBR test at 95% R_C of MSW sample; and (b) variation of CBR values with increase in percentage of R_C of MSW samples at 5	141

	mm deformation	
4.9	Variation of shear strength with increase in percentage of R_c of MSW samples at different confining pressure (σ_c)	143
4.10	Compaction curves for MSW fines and MSW fines mixed with different fiber content	146
4.11	(a) Variation of void ratio (e) Vs log of vertical stress (σ_v) (b) Change in void ratio (e) with fiber content (FC)	149
4.12	(a) Compression index (C_c) variation with stress range for all FC (b) Compression index (C_c) variation with fiber content (FC)	150
4.13	(a) Determination of C_v through a logarithm of time method (b) square root of time method at σ_v (800 kPa)	154
4.14	Coefficient of consolidation (C_v) variation with vertical stress (σ_v) for all FC by (a) logarithm of time method (b) square root of time method and (c) computational method	155
4.15	Shear strength variations with FC at different confining pressure	157
4.16	Stress-strain variation of fiber-induced MSW fines	158
4.17	Strength Ratio variations with FC at different confining pressure	158
4.18	(a) Mobility of cohesion (c); and (b) friction angle (ϕ) with axial strain for MSW fines (0% fiber content) and optimum fiber content (8% fiber content)	159
4.19	Stress-strain behaviour of the unreinforced and reinforced MSW fines with fibers under confining pressure of (a) 50 kPa (b) 100 kPa (c) 150 kPa	161
4.20	Typical test result plots at $\gamma=1.5\%$, $f=1$ Hz, $\sigma'_c = 100$ kPa and $R_c=90\%$: (a) deviator stress (q) versus number of cycles (N); (b) excess pore water pressure ratio (r_u) versus number of cycles (N); (c) mean effective stress (p') versus number of cycles (N)	164
4.21	Typical test result plots at $\gamma=1.5\%$, $f=1$ Hz, $\sigma'_c = 100$ kPa and $R_c=98\%$: (a) deviator stress (q) versus number of cycles (N); (b) excess pore water pressure ratio (r_u) versus number of cycles (N); (c) mean effective stress (p') versus number of cycles (N)	165
4.22	Typical test result plots at $\gamma=1.5\%$, $f=1$ Hz, $\sigma'_c = 50$ kPa and $R_c=98\%$: (a) deviator stress (q) versus number of cycles (N); (b) excess pore water pressure ratio (r_u) versus number of cycles	166

	(N); (c) mean effective stress (p') versus number of cycles (N)	
4.23	Typical test result plots at $\gamma=1.5\%$, $f=0.3$ Hz, $\sigma'_c = 100$ kPa and $R_c=90\%$: (a) deviator stress (q) versus number of cycles (N); (b) excess pore water pressure ratio (r_u) versus number of cycles (N); (c) mean effective stress (p') versus number of cycles (N)	167
4.24	Typical test result plots at $\gamma=0.6\%$, $f=1$ Hz, $\sigma'_c = 100$ kPa and $R_c=90\%$: (a) deviator stress (q) versus number of cycles (N); (b) excess pore water pressure ratio (r_u) versus number of cycles (N); (c) mean effective stress (p') versus number of cycles (N)	168
4.25	Typical test result plots at $\gamma=1.5\%$, $f=1$ Hz, $\sigma'_c = 100$ kPa and $R_c=90\%$: (a) deviator stress (q) versus axial strain (ϵ); (b) deviator stress (q) versus mean effective stress (p')	170
4.26	Typical test result plots at $\gamma=1.5\%$, $f=1$ Hz, $\sigma'_c = 100$ kPa and $R_c=98\%$: (a) deviator stress (q) versus axial strain (ϵ); (b) deviator stress (q) versus mean effective stress (p')	170
4.27	Typical test result plots at $\gamma=1.5\%$, $f=1$ Hz, $\sigma'_c = 50$ kPa and $R_c=98\%$: (a) deviator stress (q) versus axial strain (ϵ); (b) deviator stress (q) versus mean effective stress (p')	171
4.28	Typical test result plots at $\gamma=1.5\%$, $f=0.3$ Hz, $\sigma'_c = 100$ kPa and $R_c=90\%$: (a) deviator stress (q) versus axial strain (ϵ); (b) deviator stress (q) versus mean effective stress (p')	171
4.29	Typical test result plots at $\gamma=1.5\%$, $f=0.3$ Hz, $\sigma'_c = 100$ kPa and $R_c=90\%$: (a) deviator stress (q) versus axial strain (ϵ); (b) deviator stress (q) versus mean effective stress (p')	172
4.30	Effect of relative compaction (R_c) on liquefaction potential of compacted MSW fines	174
4.31	Effect of effective confining pressure (σ'_c) on liquefaction potential of compacted MSW fines	175
4.32	Variation of (a) dynamic shear modulus (G); and (b) damping ratio (D) with number of cycles (N) for different frequency (f), variation of (c) dynamic shear modulus (G); and (d) damping ratio (D) with frequency (f) for different R_c corresponding to $\sigma'_c = 100$ kPa and $\gamma=1.5\%$	176
4.33	Variation of (a) dynamic shear modulus (G); and (b) damping ratio (D) with number of cycles (N) for different σ'_c , variation of (c) dynamic shear modulus (G); and (d) damping ratio (D) with σ'_c for different R_c corresponding to $f=1$ Hz and $\gamma=1.5\%$	178
4.34	Variation of (a) dynamic shear modulus (G); and (b) damping ratio (D) with number of cycles (N) for different R_c , variation of	180

	(c) dynamic shear modulus (G); and (d) damping ratio (D) with R_c corresponding to $f=1$ Hz, $\sigma'_c = 100$ kPa, and $\gamma=1.5\%$	
4.35	Variation of (a) dynamic shear modulus (G); and (b) damping ratio (D) with the shear strain (γ) for different R_c corresponding to $\sigma'_c = 100$ and $f=1$ Hz, variation of (c) dynamic shear modulus (G); and (d) damping ratio (D) with the shear strain (γ) for different σ'_c corresponding to $f=1$ Hz and $R_c =96\%$, variation of (e) dynamic shear modulus (G); and (f) damping ratio (D) with the shear strain (γ) for different frequency (f) corresponding to $R_c =96\%$ and $\sigma'_c = 100$	182
4.36	Degradation index plot with respect to number of cycles for different relative compaction (R_c) at (a) $f=1$ Hz, $\sigma'_c=100$ kPa, $\gamma=0.6\%$ (b) $f=1$ Hz, $\sigma'_c=100$ kPa, $\gamma=1.5\%$	186
4.37	Degradation index plot with respect to number of cycles for different effective confining pressure (σ'_c) at (a) $f=1$ Hz, $\gamma=0.6\%$, $R_c=98\%$ (b) $f=1$ Hz, $\gamma=1.5\%$, $R_c=98\%$	186
4.38	Degradation index plot with respect to number of cycles for different shear strain (γ) at (a) $f=1$ Hz, $\sigma'_c =100$ kPa, $R_c=90\%$ (b) $f=1$ Hz, $\sigma'_c =100$ kPa, $R_c=98\%$	187
4.39	First cycle hysteresis loop for different FC (a) at $\gamma=1.5\%$ (UU condition) (b) $\gamma=0.6\%$, (c) $\gamma=0.9\%$, and (d) $\gamma=1.2\%$ for CU condition	189
4.40	Variation of dynamic shear modulus (G) with no. of loading cycles (N) for (a) at $\gamma=1.5\%$ (UU condition) (b) $\gamma=0.6\%$, (c) $\gamma=0.9\%$, and (d) $\gamma=1.2\%$ for CU condition. (e) G (for first cycle) variation with FC at different γ	190
4.41	Degradation index variation with no. of loading cycles (N) for (a) at $\gamma=1.5\%$ (UU condition) (b) $\gamma=0.6\%$, (c) $\gamma=0.9\%$, and (d) $\gamma=1.2\%$ for CU condition	192
4.42	Variation of damping ratio (D) with no. of loading cycles (N) for (a) at $\gamma=1.5\%$ (UU condition) (b) $\gamma=0.6\%$, (c) $\gamma=0.9\%$, and (d) $\gamma=1.2\%$ for CU condition. (e) G (for first cycle) variation with FC for different γ	193
4.43	Excess PWP ratio (r_u) variations with FC at (a) $\gamma=0.6\%$, (b) $\gamma=0.9\%$, and (c) $\gamma=1.2\%$. Variation of r_u with N at (d) 0% FC (e) 8% FC for different γ	196
4.44	Input-output wave response for (a) unconfined unsaturated MSW fine sample at MDD (b) unsaturated (UU) sample of MSW fine at σ_c (100 kPa) (c) saturated (UU) sample of MSW fine at σ'_c (100 kPa) at different excitation frequencies. (d) Input-output wave response at different FC for unsaturated	199

MSW fine sample at σ_c (100 kPa) and f (1kHz)

4.45	Shear wave velocity (V_s) variations with excitation frequency (f) for (a) different fiber content (FC) (b) different relative compaction (R_c)	201
4.46	Shear wave velocity (V_s) variation with confining pressure (σ_c) for different excitation frequencies (f) at fiber content (FC) of (a) 0% (b) 0.5% (c) 1% (d) 2% (e) 4% (f) 8% (g) 10%	203
4.47	Shear wave velocity (V_s) variation with fiber content (FC) at excitation frequency (f) of (a) 0.5 kHz (b) 2 kHz. (c) Variation of G_R/G_{UR} ratio with FC for different excitation frequencies and confining pressure	207
4.48	Shear wave velocity (V_s) variation with (a) excitation frequency (f) (b) relative compaction (R_c) at f (1.5kHz), for the MSW fine sample at MDD at UU and CU conditions	208
4.49	Comparative past studies of small strain shear modulus (G_{max}) with fiber content (FC). (1-(Alidoust et al., 2018); 2-(Li and Senetakis, 2017); 3-(Claria and Vettorelo, 2016))	210
5.1	(a) Curves for r_u versus N/N_L ($\gamma=0.6\%$). Comparisons between experimental and model predicted results for (b) $\gamma=0.6\%$, (c) $\gamma=0.9\%$, and (d) $\gamma=1.2\%$	215
5.2	Correlation between G_R/G_{UR} and τ_R/τ_{UR}	219
5.3	Typical variation of dissipated energy/unit volume per cycle until liquefaction of MSW fines sample at $R_c=90\%$ tested at $f=1$ Hz, $\gamma=0.6\%$ and $\sigma'_c=100$ kPa	222
5.4	Typical variation of cumulative energy/unit volume per cycle until liquefaction of MSW fines sample at $R_c=90\%$ tested at $f=1$ Hz, $\gamma=0.6\%$ and $\sigma'_c=100$ kPa	222
5.5	Variation of cumulative dissipated energy with cyclic shear strain (γ) of MSW fines specimen representing effect of relative compaction (90 to 98%), effective confining pressure (50 kPa, 70 kPa and 100 kPa), loading frequency (1 Hz, 0.5 Hz and 0.3 Hz)	223
5.6	Variation of predicted values of dissipated energy of MSW fines with the observed experimental results	224
5.7	Variation of cumulative dissipated energy with cyclic shear strain (γ) and fiber content (FC)	225
5.8	Variation of normalised cumulative dissipated energy ($\Delta W_R/\Delta W_{UR}$) with normalised factor 'm' (FC/γ)	226
5.9	Correlation plot of $G/G_{max} - \log \gamma$ for MSW fines (considering the loading frequency (0.3, 0.5, and 1Hz) and effective confining pressure (50, 70, and 100 kPa) at relative compaction of (a) 90% (b) 92% (c) 94% (d) 96% and (e) 98%	227

5.10	Correlation plot of $G/G_{max} - \log \gamma$ for fiber-reinforced MSW fines (considering the loading frequency of 1Hz, effective confining pressure of 100 kPa and density of 1.51g/cc at all the fiber content (0 to 10%))	231
5.11	Correlation plot of $D - \log \gamma$ for MSW fines (considering the loading frequency (0.3, 0.5, and 1Hz) and effective confining pressure (50, 70, and 100 kPa) at relative compaction of (a) 90% (b) 92% (c) 94% (d) 96% and (e) 98%	232
5.12	Correlation plot of $D - \log \gamma$ for fiber reinforced MSW fines (considering the loading frequency of 1Hz, effective confining pressure of 100 kPa and density of 1.51g/cc at all the fiber content (0 to 10%))	235
6.1	Machine learning model	242
6.2	Constitution of an artificial neurons	244
6.3	Prediction of dynamic shear modulus for (a) Unreinforced MSW fines, and (b) Fiber reinforced MSW fines using ANN model	249
6.4	Prediction of dynamic shear modulus for (a) Unreinforced MSW fines, and (b) Fiber reinforced MSW fines using GPR model	250
A.1	Geosynthetics used in the study (a) Geotextile, and (b) Geonet	318
A.2	Flow chart of the testing program considered for the present study	320
A.3	Geosynthetics arrangements considered for the study	321
A.4	Sample images (a) 1-layer reinforcement, (b) 2-layers reinforcement, and (c) 3-layers reinforcement before failure, and failure pattern images of sample for (d) 1-layer geotextile reinforcement, (e) 2-layers geotextile reinforcement, (f) 3-layers geotextile reinforcement, (g) 1-layer geonet reinforcement, (h) 2-layers geonet reinforcement, and (i) 3-layers geonet reinforcement at confining pressure of 150 kPa	322
A.5	Deviator stress variation with number of reinforcement layers for (a) Geotextile, and (b) Geonet at confining pressure of 150 kPa	324
A.6	Peak shear strength variation with number of reinforcement layers for (a) Geotextile, and (b) Geonet for varying confining pressures (50,100 and 150 kPa)	325
A.7	Mohr circles for unreinforced and reinforced (a) Geotextile, and (b) Geonet at confining pressure of 150 kPa	326

A.8	Average shear strength comparison of geotextile and geonet	326
A.9	Comparison of present study (a) cohesion (c), and (b) friction angle (ϕ) with other composite reinforced studies. (Note: ¹ (Fiber reinforced MSW fines (Present study); ² (Maher and Ho 1993); ³ (Noorzad and Mirmoradi 2010); ⁴ (Ram Rathan Lal and Mandal 2013); ⁵ (Chen et al. 2014); ⁶ (Benessalah et al. 2016); ⁷ (Dasaka and Sumesh 2011).))	327
A.10	Deviator stress vs axial strain plot (10 cycles) for (a) unreinforced (b) 1-layer geotextile (c) 2-layers geotextile (d) 3-layers geotextile (e) 1-layer geonet (f) 2-layers geonet, and (g) 3-layers geonet	333
A.11	Comparison of hysteresis loop (1 st cycle) for unreinforced and (a) geotextile reinforced, and (b) geonet reinforced MSW fines	335
A.12	Dynamic shear modulus (G) variation with number of cycle (N) for unreinforced and (a) geotextile reinforced, and (b) geonet reinforced MSW fines, and Damping ratio (D) variation with number of cycle (N) for unreinforced and (c) geotextile reinforced, and (d) geonet reinforced MSW fines	319
A.13	(a) Deviator stress improvement with reinforcement layers (static loading conditions) (b) Deviator stress reduction with reinforcement layers (cyclic loading conditions), and (c) strength ratio ($SR_{S/D}$) with number of reinforcement layers	338

LIST OF TABLES

Table No.	Description	Page No.
2.1	The categories to evaluate the objectives of Landfill Mining projects	20
2.2	Characterization of the excavated landfill waste	30
2.3	Screen size considered for the segregation in past projects	35
2.4	Metal concentrations found in MSW fine fractions of landfills (Conc. in mg/kg dry weight)	43
2.5	Global standards for heavy metals concentration limits in soils/composts (Conc. in mg/kg)	46
2.6	Physico-chemical characteristics of the MSW fine fraction (water extract) for a few Indian landfill sites	48
2.7	Geotechnical properties of MSW	63
2.8	Effect of different parameters on the dynamic properties of municipal solid waste (Source @ Zekkos et al., 2008)	70
3.1	Experimental testing program for physical, chemical, morphological, and geotechnical characteristics	100
3.2	Standards used for different laboratory tests	101
3.3	Testing program for MSW fines under cyclic loading condition (Cyclic triaxial test)	112
3.4	Testing program for fiber-reinforced MSW fines under cyclic loading condition (Cyclic triaxial test)	115
3.5	Specification of cyclic triaxial test equipment	117
4.1	List of compounds present in MSW fines	132
4.2	Summarized chemical characteristics of MSW landfills in India	134
4.3	Variation of unconfined compressive strength (q_u) and cohesion (c) with increase in Maximum Dry Density (%)	142
4.4	Variation of cohesion and angle of internal friction with increase in R_C of MSW fines	143
4.5	Summarized geotechnical characteristics of MSW fines	144
4.6	Settlement analysis with fiber content	149

4.7	Percentage change in compression index (C_c) between reinforced and unreinforced MSW fines	150
4.8	Maximum values for coefficient of consolidation (C_v)	152
4.9	Variation of strength parameters with fiber content	156
4.10	Shear strength parameters for unreinforced and reinforced MSW fines with fibers under different triaxial conditions	160
4.11	Effect of different parameters on the dynamic properties of MSW fine fractions and sand	184
4.12	R_c effect on V_s at different confining pressures and excitation frequencies	202
5.1	Nonlinear fittings for the parameters a , b , b_1 , and c used in the r_u (excess pore water pressure ratio) model	217
5.2	Nonlinear fittings for the parameters A , B , C , and D used in the cubic polynomial model	219
5.3	Hyperbolic model parameters and R^2 values for the fitted normalized shear modulus (G/G_{max}) vs. $\log \gamma$ correlation at different R_c	230
5.4	Model parameters and R^2 values for the fitted damping ratio vs. shear strain correlation at different R_c	232
6.1	Machine learning application for MSW model prediction	240
6.2	Root Mean Squared Error (RMSE) values obtained from prediction model analysis	251
6.3	Sensitivity indices for the first-level interactions	252
A.1	Properties of the reinforcing material used	318
A.2	Strength ratio values obtained from the experimental study	330
A.3	Variation of dynamic shear strength parameter with the number of reinforcement layers	337

NOMENCLATURE

AASHTO- American association of state highway and transportation officials

AI- Artificial intelligence

ANN- Artificial neural network

B- Skempton's pore pressure parameter

BE- Bender element

BPNN- Backpropagation neural network

c- Cohesion

C&D- Construction and demolition

C.C.- Cross-correlation

CBR- California bearing ratio test

Cc- Coefficient of curvature

C_c - Compression index

CD- Consolidated drained

CIF- Central instrument facility

CIPET- Central institute of plastic engineering and technology

COD_d- Dissolved chemical oxygen demand

COD_t- Total chemical oxygen demand

CPCB- Central pollution control board

CPT- Cone penetration test

CSR- Cyclic stress ratio

CTX- Cyclic triaxial

Cu- Coefficient of uniformity

CU- Consolidated undrained

C_v - Coefficient of consolidation

D- Material damping ratio

DI- Deionized

DOC- Dissolved organic carbon

DS- Direct shear

DSS- direct simple shear

DST- Direct shear test

e- Void ratio

EDTA- Ethylene diamine tetra acetic acid

EDX- Energy dispersive x-ray

ELFM- Enhanced landfill mining

ELV- End of the life vehicle

EPR- Evolutionary polynomial regression

f - Loading frequency

FAO- Food and agriculture organization

FC- Fiber content

FL- Fiber length

G- Secant/ dynamic shear modulus

G/G_{\max} - Normalized shear modulus reduction

GDP- Gross domestic product

G_{\max} - Small strain shear modulus

GP- Genetic programming

GPR- Gaussian process regression

GRU- Gate recurrent unit

G_s - Specific gravity

HDPE- High density polyethylene

INDOT -Indiana department of transportation

IRC- Indian road congress

IS- Indian standard

IW- Industrial waste

k- Coefficient of permeability

kN- Kilo newton

kPa- Kilopascal

LBR- Laboratory leach bed reactors

LFM- Landfill mining

LFMSF -landfill-mined soil fraction

LSTM- Long short-term memory

MAM- Microtremor analysis method

MASW- Multichannel analysis of surface waves

MBT- Mechanically biologically treated

MC -Moisture content

MDD- Maximum dry density

MICP -Microbiologically induced calcium carbonate precipitation

ML- Machine learning

ml- Millilitres

MNRE- Ministry of new and renewable energy

MoEF &CC- Ministry of environment, food, and climate change

MPa- Megapascal

MSW- Municipal solid waste

MSWC -MSW compost

MT- Million metric tonnes

N- Number of cycles

NJDEP -New jersey department of environmental protection

N_L -Initial cycles of liquefaction

NP- Non-plastic

NTPC- National thermal power corporation limited

OMC- Optimum moisture content

P.P.- Peak-to-peak

p' - Mean effective stress

PAH- Polycyclic aromatic hydrocarbons

PCC- Pollution control committees

PETE- Polyethylene terephthalate

PI- Plasticity index

PWP- Pore water pressure

q - Deviator stress (dynamic loading case)

q_{\max} - Maximum deviator stress

q_u - Unconfined compressive strength

R- Reinforced

RBF- Radial basis function

RC- Resonant column

RCTS- Resonant column torsional shear

RDCSCC- Residential direct contact soil clean up criteria

RDF- Refuse-derived fuel

RE- Reinforced earth

REEs- Rare earth elements

RNN- Recurrent neural network

r_u - Excess PWP (pore water pressure) ratio

S.S.- Start-to-start

SASW- Spectral analysis of surface waves

SEM- Scanning electron microscope

SEPA- Swedish environmental protection agency

SLM- Soil-like material

SM- Silty sand

SPCB- State pollution control board

SPT- Standard penetration tests

SR- Strength ratio

SS- Simple shear

SVM- Support vector machine

SWM- Solid waste management

TDS- Total dissolved solids

TOC- Total organic carbon

TPD- Tonnes per day

TX- Triaxial

UCS- Unconfined compression test

UR- Unreinforced

US TCLP- United states toxicity characteristic leaching procedure

USCS- Unified soil classification system

USEPA- United states environmental protection agency

UU- unconsolidated undrained

V_p - Compression wave velocity

V_s - Shear wave velocity

WST- Weight sounding test

WtE- Waste-to-energy

XRD- X-ray diffraction

XRF- X-ray fluorescence

Δu = Change in pore pressure

ΔW - Dissipated energy/ unit volume

$\Delta \sigma_c$ = Change in confining pressure

λ - Wavelength

ρ - Material density

δ - Degradation index

ε - Axial strain

ϕ - Internal friction/ Angle of friction

γ - Shear strain

μm - micrometer

σ'_c =Effective confining pressure

σ_c - Confining pressure

σ_d - Deviator stress (static loading case)

σ_v - vertical stress

τ - Shear strength